J. Mol. Model. **2000**, *6*, 477 – 490

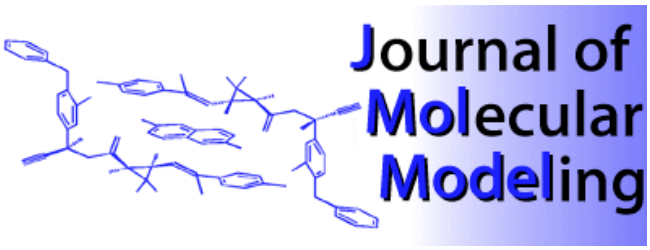

FULL PAPER

Molecular Modelling of Helix Stability in Carrageenans

Naseem A. Ramsahye and Brendan J. Howlin

Department of Chemistry, School of Physics and Chemistry, University of Surrey, Guildford, Surrey, GU2 7XH, United Kingdom. E-mail: b.howlin@surrey.ac.uk

Received: 7 October 1999/ Accepted: 17 December 1999/ Published: 27 June 2000

Abstract Molecular models of disaccharides, and single and double helices up to eight monomers in length have been constructed of the two types of glycosidic linkage in the carrageenan chain. These links are a galactose to anhydrogalactose link (GA link), and an anhydrogalactose to galactose link (AG link). These models are also based on κ-carrageenan, which contains a 4-sulphate galactose ring. The effects of the sulphate groups on the conformation of the helices may be seen by the angles of φ and ψ explored during the simulations by the AG and GA linkages. It has been observed that the molecule can explore a greater area of conformational space about the GA link than the AG link. This could be due to steric hindrance caused by the bulky sulphate group near the AG link. The sulphate group is further away from the GA link than from the AG link, and this may provide a possible explanation for the relatively unhindered movement about the GA link compared to the AG link. The results have also shown that the conformational space for the AG linkages, as well as the GA linkages vary between different lengths of the polysaccharide chain. Single helix models show little stability in molecular dynamics simulation, whereas the eight monomer double helix model is more stable than a six monomer double helix model.

Keywords Carbohydrate, Carrageenans, Molecular dynamics

Introduction

Carbohydrates are polyhydroxy aldehydes and ketones. They are among the most abundant organic compounds in nature, found in both plants and animals. Carbohydrates are sources and stores of energy, and can be divided into two broad groups: sugars and polysaccharides. The simplest sugars are monosaccharides and a disaccharide can be formed *via* the combination of two monosaccharides with the elimination of water [1,2]. Polysaccharides are polymeric substances consisting of 10's, 100's or even 1000's of monosaccharides [2]. They have found many uses in various industries. Cellulose is the most abundant polysaccharide, and is used in the paper industry (in the form of wood pulp), and in the manufacture of flexible films, rayons and certain plastics [3]. More complex polysaccharides are involved in the bacterial cell wall, connective tissue and blood group substances, as well as natural lubricants and gums [1]. Cereals and crops such as potatoes contain starch, the main polysaccharide for food consumption. Other uses have been found in the pharmaceutical, food and cosmetic industries [3]. Polysaccharides can be obtained from seaweeds, and examples of these include agarose and carrageenan, which are used in the food industry as emulsifiers, stabilisers and gelling agents.

Correspondence to: B. J. Howlin

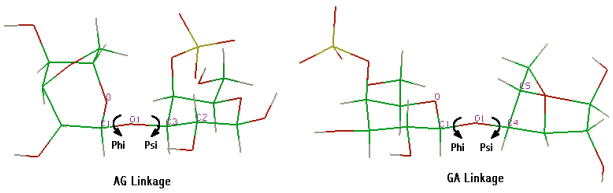

Figure 1 *The AG linkage (left) and the GA linkage (right) showing the φ and ψ angles*

Carrageenans are from a class of polysaccharides called galactan polysaccharides, which occur in numerous species of red seaweed. Carrageenans are mainly used in industry as food additives, and indeed, it has been said that they are more versatile for this purpose than agars. Carrageenans have been used as emulsifying and thickening agents and also as stabilisers in foods such as milk products, flans, chocolate, ice creams, low fat spreads and dessert gels (for gelation). One important characteristic of carrageenan which allows its use in foods is the fact that it forms gels at moderate temperatures [4]. Carrageenans are polysaccharides made up of alternating ®-1,3 and α-1,4 linked galactose residues. The 1,4 linked residue is usually present as anhydrogalactose. There are various forms of carrageenan, including κ-, ι- and λ-carrageenan. The positions and numbers of sulphate groups in the structures vary between the various forms. Figure 1 shows κ-carrageenan, which contains a 4-sulphate galactose ring [5].

There are two types of glycosidic linkage in the carrageenan chain, a galactose to anhydrogalactose link (GA link), and an anhydrogalactose to galactose link (AG link), both of which are shown in Figure 1. Each link has two torsion angles, φ and ψ. These are also defined in Figure 1.The carbon atoms are represented as green, the hydrogen atoms are grey, the oxygen atoms are red and the sulphur atoms are yellow. For the AG linkage, the φ angle was measured using the atoms O, C1, O1, and C3, as labelled in Figure 1. ψ for the AG linkage was measured using C1, O1, C3 and C2. For the GA linkage φ was measured using O, C1, O1 and C4. ψ was measured using C1, O1, C4 and C5. Carrageenans differ from agarose in that they contain sulphate groups, and that the galactose sugar ring is in the D form, whereas it is in the L form in agarose. Carrageenans can be induced to crystallise and Rees et al. [6] have determined the unit cell parameters of ι-carrageenan as follows: a = b = 1.373 nm, c = 1.328 nm, α= ® = 90°, γ= 120°. Carrageenans form helices when cooled to a sufficient temperature (like agarose, gellan and certain other polysaccharides). These helices can then combine to form double helices, and it is accepted that aggregation of these double helices causes the formation of the gel network [4]. According to Morris et al. [7-8], the double helices form junction zones between the chains of monomers. This results in the formation of soluble clusters (domains), which combine to form a network through the interaction of the helices from different domains. It is believed that these interactions participate in the gel formation mechanism. The domains are

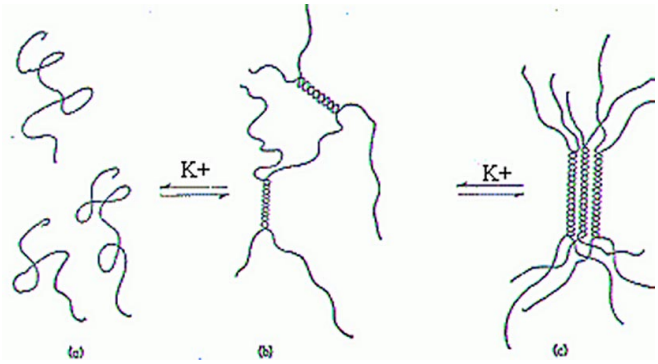

Figure 2 *Diagram (a) shows the random chains, (b) shows the helices, (c) shows the aggregation of the helices. The presence of potassium ions, K^+, promotes the gelation process*

usually ordered, or aggregated in the presence of cations. Cations such as potassium ions are said to favour the gelation process [9]. Figure 2 illustrates the transition from random coil to helix to domain structure [10].

It has been said by Rees [11] that sulphated compounds enter solution more easily than unsulphated compounds, due to the fact that the negative sulphate groups can interact with the partially positive hydrogen atom in the water molecules. This implies that as carrageenan has sulphate groups, aggregation of carrageenan helices is less favourable than that of agarose, since aggregation of the double helix network is the opposite of entering the solution phase [11]. Previous work by us on Gellan [12] and Agarose [13] has demonstrated the efficacy of using molecular modelling to investigate the conformational flexibility of model carbohydrate systems. Others workers have used carbohydrate modelling to show that computer simulation is the best means of confirming a structural model of a glycosphingolipid derived from NMR (Kawakami et. al. [14]). Also the conformational behaviour of two hexasaccharides has been probed by molecular dynamics simulation by Kozar et. al. [15] and recently a carbohydrate modelling tool (SWEET) has appeared on the Internet (Bohne et. al. [16]). This work extends our previous experience to the more complicated sulphated carrageenan system.

Methodology

The simulations and calculations performed were similar to those performed by Haggett et al. [13] on agarose, except that only the implicit solvent case was considered. The models were built using MSI's INSIGHTII [17] software running on a Silicon Graphics Indigo XZ4000 computer. Discover v2.95 [17] was used to perform the minimisation and the molecular dynamics calculations. The AMBER forcefield with Homans' [18] modification for use with polysaccharides was the forcefield used in all the calculations. The AMBER forcefield is widely used for carbohydrate simulation, e. g.

Table 1 *φ and ψ values showing the positions of minima for the AG link*

	Positive φ Region		Negative φ Region	
	φ (°)	ψ (°)	φ (°)	ψ (°)
1 monomer	71.8	-144.0	-71.8	-144.0
3 monomers	71.5	-108.0	71.9	-72.2
6 monomers	71.7	-144.1	-72.1	-144.0
8 monomers	144.0	-71.6	-180.0	35.7

Gruza et al. [19] have used it to produce reliable furanose models, Martin Pastor et. al. [20] have used a variety of methods to fit to NMR solution data in lactose modelling and concluded that the AMBER/Homans method was in reasonable agreement. The helices were built up from the disaccharide units, using φ and ψ angles used by Haggett et al. [13] for the AG and GA linkage. These were: AG Link: φ = -52.2°, ψ = 156.8°, GA Link: φ = -123.9°, ψ = -113.2°.

Analysis of dihedral angles

Two torsion angles, φ and ψ, were defined (see Figure 1) and kept fixed in space while the rest of the molecule was allowed to minimise. A dielectric constant of 80 was used, so as to simulate the minimisation in water. The data was extracted and plotted as a φ/ψ map using INSIGHTII, and Microsoft Excel. The minimisation was run for both the GA and AG linkages separately, for chain lengths of one, three, six and eight monomers. Two minimisation algorithms were used: steepest descents for 1000 iterations, and then conjugate gradients for 100 iterations, to meet a convergence criteria of less that 0.01 kcal $mol^{-1}A^{-1}$.

Conditions for dynamics

The system was warmed to 300K for 100 iterations in steps of 1 iteration, where 1 iteration = 1 femtosecond. Depending on whether a double helix or single helix was being simulated, the molecular dynamics simulation was run for 100000 iterations (single helices) or 50000 iterations (double helices) using the Verlet integration method [21] The reason for this is the time it takes to run molecular dynamics on a large molecule under periodic boundary conditions (PBC) is quite large. The simulations were run for chain lengths of three, six and eight monomers with PBC applied to simulate the bulk situation. The cell size for the six monomer double helix was 40 by 20 Å. For the eight monomer double helix, the cell size was 60 by 25 Å. Only six and eight monomer chains were simulated as double helices. For the double helices, one helical chain was kept fixed in space, while the other was allowed to relax around it, and dynamics calculations were performed on this helical chain. Further simulations were run with three, four, five, six and eight monomer chains as single helices, but not with PBC applied. The cut-off distances were larger than the 15 Å used by Haggett et al. [13] and Larwood et al. [12] because a possible bug would not allow a cut-off of less than the cell dimensions, in this version of the software used. The explicit image model was used, and the large cut-offs meant that more interactions than usual were considered. However, the interactions of molecules a large distance from each other would be very small, and were considered not to have any significant effect on the actual calculation (except that it would increase the time the simulation took to complete).

Results and discussion

Analysis of dihedral angles

AG linkage Figure 3 shows the contour plot (φ *vs* ψ with energy plotted along the z-axis) for the AG linkage in one monomer i.e. a disaccharide. As can be seen from Figure 3, there is a minimum valley at around the φ value of -72°, and

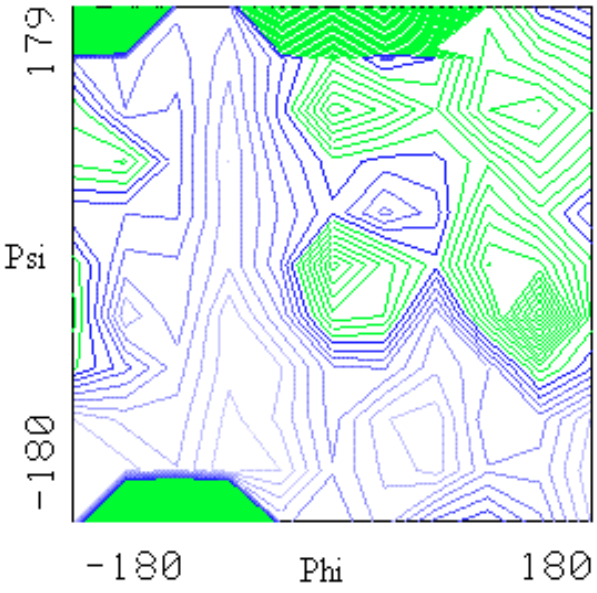

Figure 3 *A φ/ψ map for the AG link in the one monomer unit. The green areas show areas of high energy, the blue areas show low energy*

also a low energy area at a φ value of 72°. There is also a hill in between them, as shown by the contours and the green areas. The maximum height of this hill (maximum energy) occurs at around the φ value of 0°. The hill could quite easily be traversed around the region where ψ is between about -50 and -180°, as the contour is not very steep in this region. The difference in energy between the lowest point in the valley and the highest point of the hill between the ψ values of -50 and -180° is only about 4 or 5 kcal mol^{-1}. Table 1 shows the φ and ψ values for the different chains at which there are minima. The contour plots for the AG links in the other chains all have the same features as the one for the one monomer chain, i.e. two valleys and a hill in between. This grouping into two distinct minima is common in carbohydrate systems e.g. a study of the conformational flexibility of plant lectin glycosides by Gilleron et al. [22] also shows two distinct minima. As the data in Table 1 show, the minima seem to occur at values of φ = 71 or -71°. However, the hill is much bigger in the three, six and eight monomer contour plot, and traversing them would not be possible, as the contours are too steep. One reason for this could be that there are more interactions possible given the greater number of atoms and conformations of an eight monomer helix compared with that of a one monomer helix. The maxima all occur in the same area too, i.e. at φ values of around zero degrees, or more or less in the middle of the plot, bisecting the φ axis (Table 2).

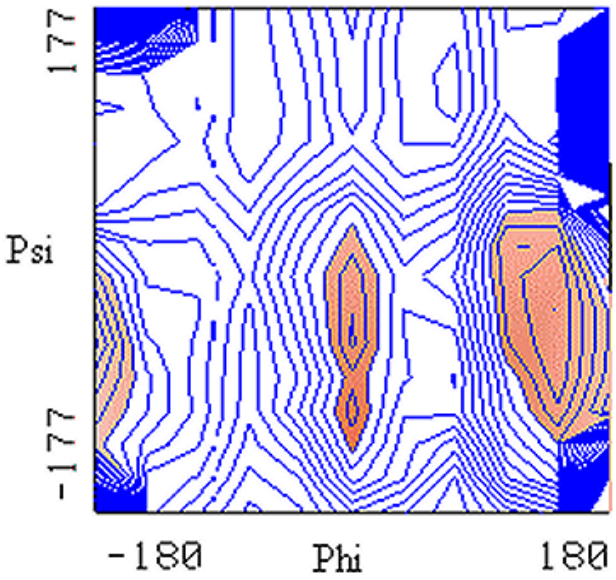

Figure 4 *The GA contour plot for a one monomer unit. Red areas show maxima*

Table 2 *φ and ψ values of the maxima in the AG link*

	φ (°)	ψ (°)
1 monomer	-1.0	-0.3
3 monomers	36.2	34.8
6 monomers	-0.5	35.6
8 monomers	36.1	-0.2

tures of the GA link in a one monomer unit. Described above are the GA and AG linkages and where the energy minima and maxima fall in conformational space. The contour plots for the eight and six monomer chains are different. The same features are present, i.e. two valley regions where the minima occur at φ values of about -72 and 72°, and a hill in the middle, around the region where φ has a value of 0°. The φ and ψ angles for both types of linkages (GA and AG) were extracted for each double helix. These were plotted as a φ-ψ plot (i.e. a Ramachandran [23] map) and the plots for each helix were compared to the contour maps for the respective links.

Table3 *φ and ψ values for GA minima*

	Positive φ Region		Negative φ Region	
	φ (°)	ψ (°)	φ (°)	ψ (°)
1 monomer	71.4	-178.9	-71.9	-179.5
3 monomers	180.8	144.4	-72.1	73.5
6 monomers	179.9	71.6	-144.2	71.9
8 monomers	180.0	71.8	-71.8	178.1

GA Linkage The GA linkage's contour map has similar features to that of the AG linkage. This means two valleys and a hill region. The positions of the minima and maxima are similar too, i.e. around φ = 72 and -72° for the minima, and φ = 0 for the maxima (Tables 3 and 4).

Although there are some minima at around φ = 180°, it should be noted that there are also minima at φ = 72° which are very similar in energy to the quoted minima, and so these are still favourable conformations. Figure 4 shows the fea-

Table4 *φ and ψ values for GA maxima*

	φ (°)	ψ (°)
1 monomer	0.1	-47.5
3 monomers	0.2	-108.3
6 monomers	-1.89	-37.6
8 monomers	0.2	-4.8

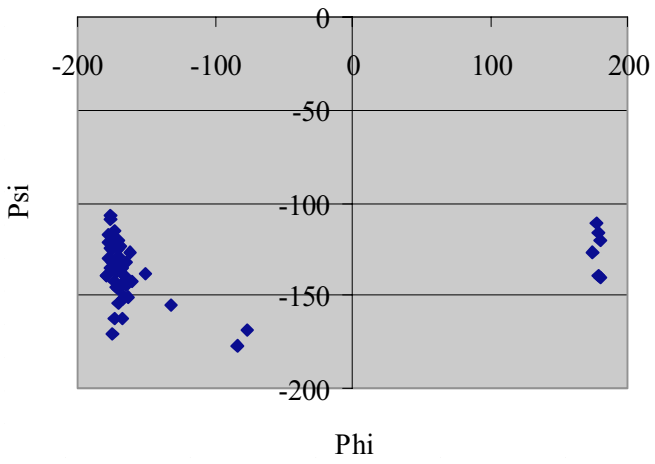

Figure 5 *The Ramachandran plot for the AG link in the eight monomer double helix*

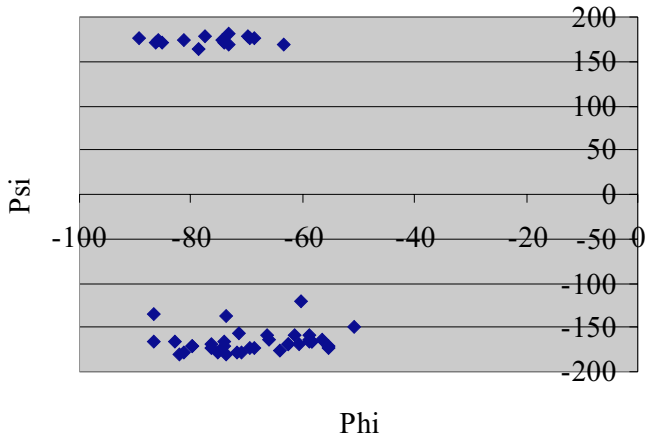

Figure 6 *The Ramachandran plot for the GA link in the eight monomer double helix*

Comparison of the Ramachandran plot of the AG link in the eight monomer double helix (Figure 5) with the contour map (See Appendices) shows that the values taken by φ and ψ fall within the valley at which the φ values are negative. The conformations taken by the helices during the simulation had φ values between -160 and -175°. There are a couple of values of φ that are positive and this conformational space is likely to have been explored near the end of the simulation for the following reason. It can be seen from the three dimensional surface plot and the contour plot (See Appendices) for the AG link in the eight monomer double helix chain, that there is a big drop in energy between the valley areas, and that there is a hill feature in between the two valleys. Therefore it would be very difficult to traverse from the area of the map where the φ values are positive to the area where φ values are negative, due to the steepness and the height of the hill.

The Ramachandran plot for the GA link is more scattered as shown in Figure 6. The preferred values of ψ seem to lie around -175° or 175°. The φ values have a bigger range, between -50° and -80°. The contour plot (See Appendices) for this link in the eight monomer chain shows that the energy difference between the various areas of the conformational space is small, and so for this reason, the molecule is allowed to explore a wider area of this space. There is a maximum in the middle of the plot, where φ and ψ are approximately zero degrees. There are also maxima around the areas where φ takes the values of 170 to 180° and -170 to -180°. This could be due to steric effects within the molecule, caused by interactions with the sulphate groups, for example. The plot for the GA link in the eight monomer double helix shows that the molecule can rotate about that link more freely than it can rotate around the AG link. This could be because the AG link is close to the bulky sulphate groups, and so could be hindered by interactions with this group upon rotation about the AG link. The Ramachandran plots for the six monomer double helix shows the same features as the plots for the eight monomer double helix (See Appendices). Much the same features occur in the plots for the six monomer AG and GA links. The AG link was more restricted in the conformational space that was allowed to be explored, and consequently in the angles of φ and ψ that the AG link in the chain was allowed to take, whereas the data for the GA link was scattered over a wider area. The contour plot for the GA link also indicated that a wider area of conformational space could be explored, as the gradients for most of the areas were not very steep, indicating little difference in energy in the space immediately nearby. The contour plots for the three monomer single helix also indicated that the helices could rotate about the GA link more freely than around the AG link. The plots for the three and six monomer chains can be found in the Appendices. However, there are marked differences between the plots for the different helices. The contour plots for the AG link for the one monomer disaccharide is not the same as the plot for the six monomer chain, or the eight monomer chain, although there are some common features present (such as the valleys and hills). The same is also true for the GA link for the different chain lengths. Previous calculations on polysaccharides have assumed that the contour plots for the AG links for different chain lengths would be the same, and the plots for the GA links for different chain lengths would be the same. However, in the case of carrageenan, this is not the case, as shown by the respective plots and the angles of φ and ψ visited by each chain during the dynamics run.

Analysis of the minimised structures

The structures were energy minimised before the molecular dynamics simulations were run. The dihedral angles were extracted. The eight monomer double helix chain AG and GA angles are plotted in Figures 5 and 6 as φ - ψ plots. The angles were measured from the energy minimised structures. Comparison with the relevant contour map for the disaccha-

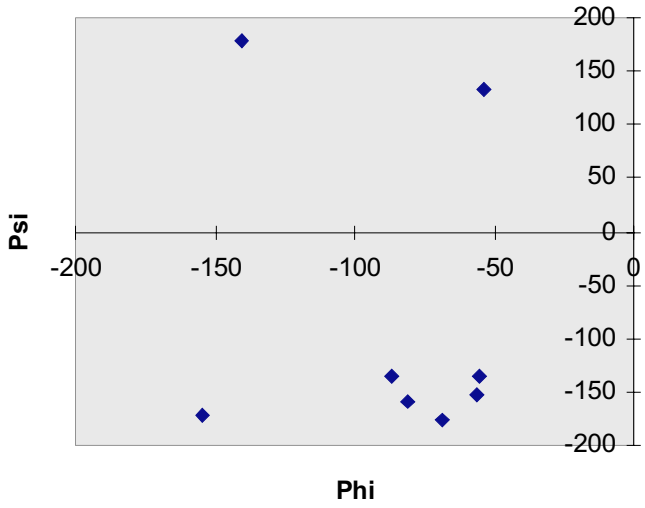

Figure 7 *The φ–ψ plot for the GA angles in the eight monomer double helix minimised structure*

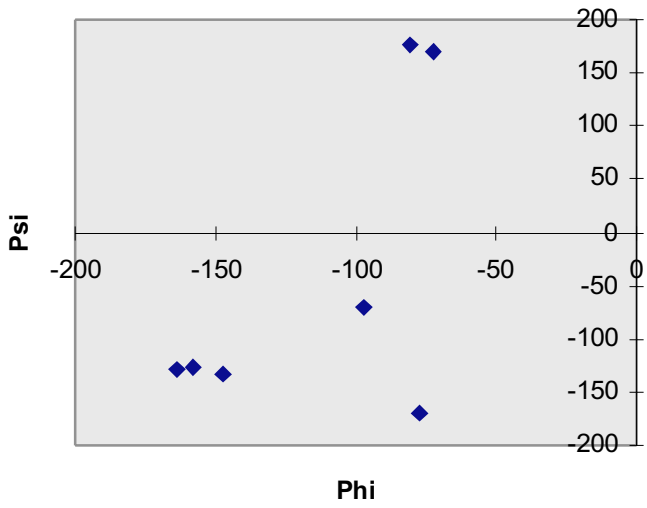

Figure 8 *The φ–ψ plot for the AG link in the eight monomer double helix minimised structure*

ride linkages shows that the angles lie in the minimum valley regions. In the case of the eight monomer chain (double helix), the minima are in the valley where the values of φ are negative (Figures 7 and 8). The plots for a single helix of eight monomers long, whether energy minimised after the dynamics simulation using PBC or not, are very similar. This may suggest that a helix of this length is stable. A visual comparison of the minimised molecule with the original model shows that there is little difference between them, further suggesting that the helices are stable. This is true of the eight monomer helix, for both double and single helices. Figure 9 shows that by looking down the helical axis, it can be seen that the eight monomer chain has kept it's double helix structure, and is not too different when compared to the original model.

Comparison of the minimised six monomer double helix chain with the original model also shows that the helices are quite stable. The minimised double helix did not lose its helical conformation. The single helix chain of this length, also retained a helical structure after minimisation. This suggests that a six monomer helix is a stable structure. Figure 10 shows that the minimised six monomer double helix keeps a helical conformation.

Looking at a single helix of only three monomers in length (Figure 11), it can be seen that a helix of this length is not at all stable, as the minimised structure has completely lost its helical conformation. However, the φ and ψ values for this minimised structure do lie in the valley regions. It should be noted, however, that the structure was minimised in implicit solvent conditions, a dielectric constant of 80 was defined. This means that there were no water molecules present in the model to interact with the chain. If there were water molecules present, they may have interacted with the chain, and helped it to keep its helical conformation. Conversely, the water molecules may also have disrupted the helical structure.

Figure 9 *The minimised eight monomer double helix (right) compared with the unminimised one (left). This is a view looking down the helical axis*

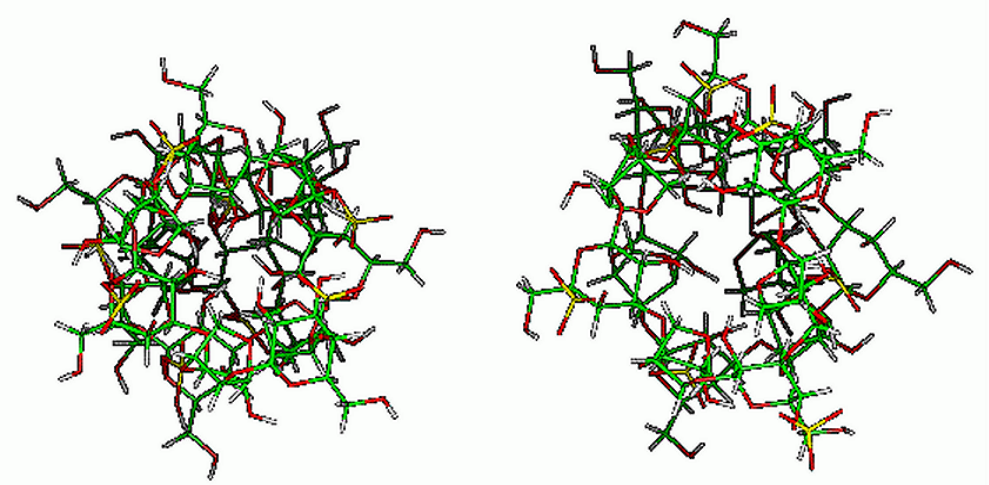

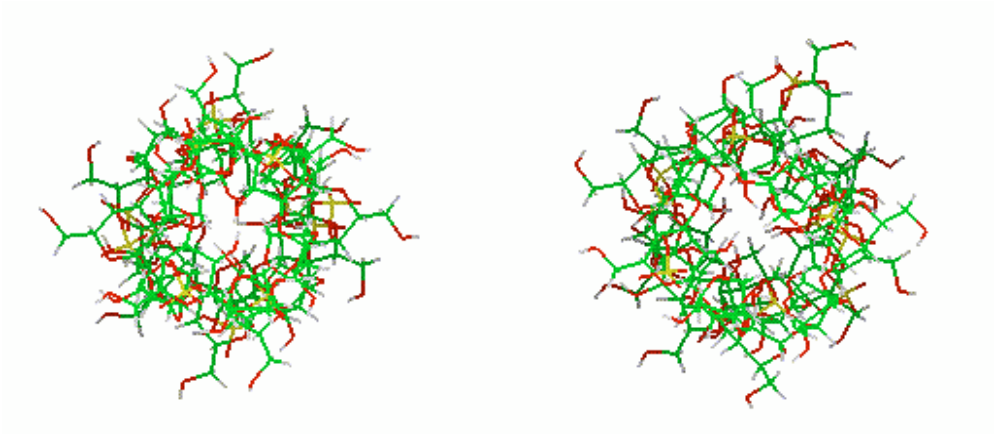

Figure 10 *The six monomer double helix, not minimised (left), and minimised (right). This is a view looking down the helical axis*

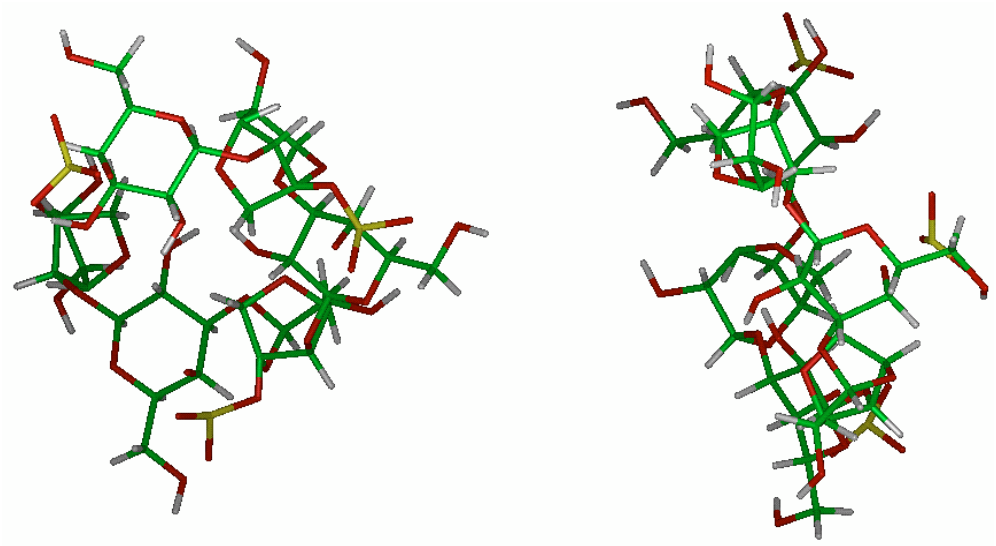

Figure 11 *The three monomer single helix, unminimised (left), and minimised (right). This is a view looking down the helical axis*

Analysis of the molecular dynamics simulations

Analysis of the three monomer single helix chain, run under PBC shows that the chain loses its helical conformation after only one picosecond. This means that the helical conformation was lost at a temperature of 289 K (below room temperature). This rapid transition to other minima occurs in other simulations of carbohydrates, e.g. Gilleron et al. [22], where transitions occur within a few picoseconds of the simulation. The time-energy plot for this chain shows two plateau regions (Figure 12).These plateaux could show regions of conformation stability, although there does not seem to be much change in the conformation between the plateaux. The chains seem to interact with other chains from neighbouring cells at the point where the plateau starts. During the dynamics run there may have been intramolecular bonding e.g. hydroxy groups interacting on the same ring. This was observed by Haggett et al. [13] for the agarose system, (three monomers, but as double helices with explicit water molecules). This may explain the structure obtained during some of the dynamics runs whereby bonds have simply formed with the sulphated galactose rings. This could mean hydrogen bond-

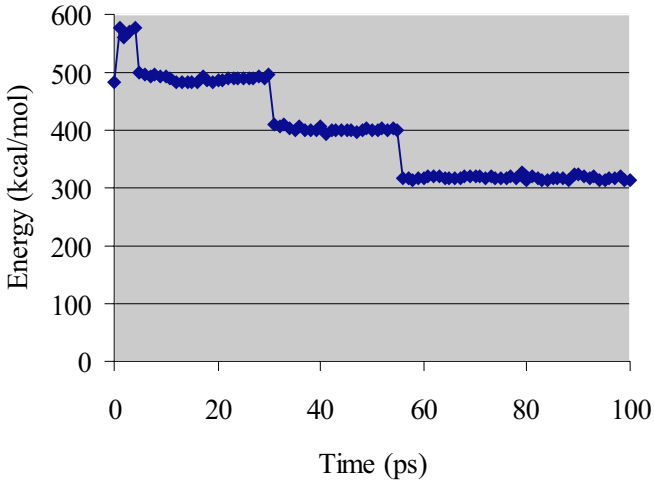

Figure 12 *The time-energy plot for a dynamics run for a three monomer single helix*

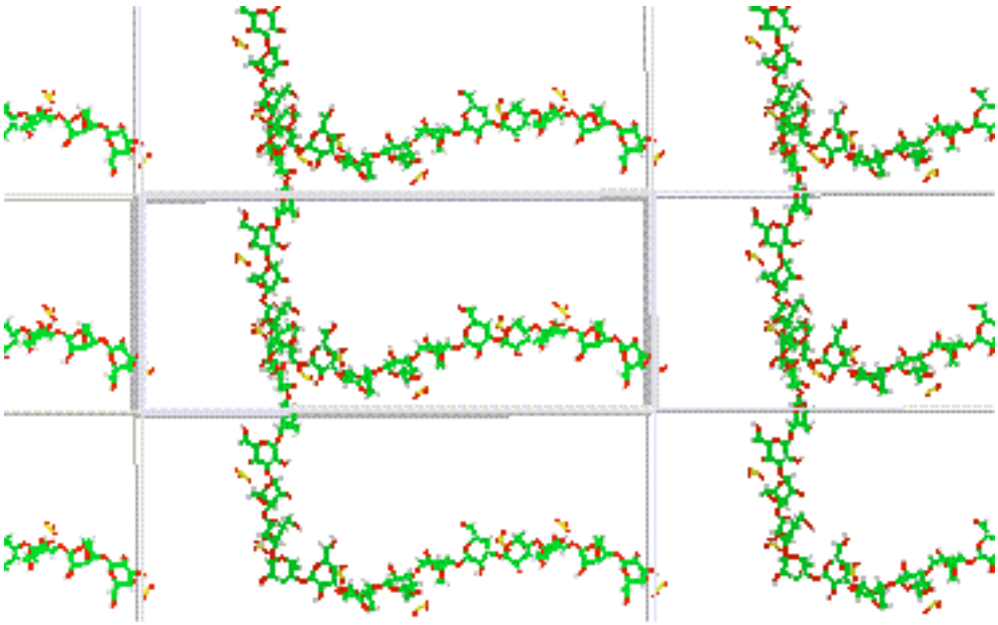

Figure 13 *The 'bent' conformation of the eight monomer single helix, interacting with neighbouring cells*

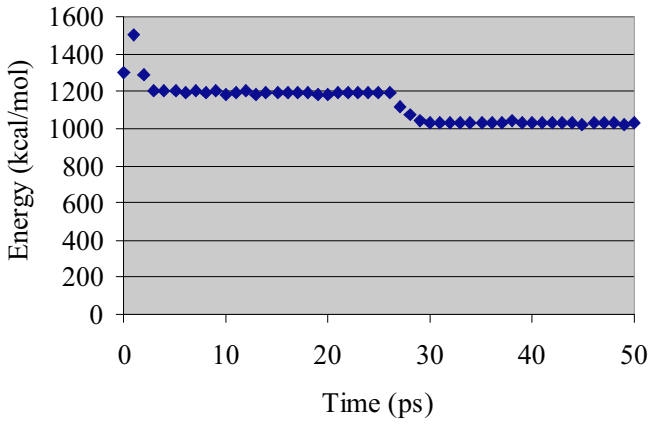

Figure 14 *The time-energy plot for a dynamics run for an eight monomer double helix*

ing between the negatively charged sulphate groups and the hydrogen atoms in the hydroxy groups. This could also be attributed to a bug in the dynamics program. This was not observed for all simulations, only the ones for single helices with no PBC applied. The results of the dynamics run for the eight monomer single helix chain shows that this chain completely unravels from a helical structure to form a straight chain after about three picoseconds, at a temperature of about 312 K. The chain is more stable than the three monomer chain, and the time energy plot for this chain shows similar features to the three monomer chain's plot, i.e. a plateau region. The eight monomer chain also adopts the same sort of conformation in that it loses its helical structure to form a single chain with a bend approximately one third of the length in from the end of the chain, as shown in Figure 13. The chain is seen to interact with other molecules in other cells. This chain also exhibited intramolecular interactions, again around the sulphated galactose rings. This run was abruptly cut short after thirty-two picoseconds due to an error in the program.

The eight monomer double helix showed some stability at the end of the dynamics run. However, the helical chain that was allowed to relax unravels into a non-helical chain at one end, and during the course of the dynamics run, this end was seen to interact with neighbouring cells. This could show the first stages of the aggregation mechanism. The time-energy plot for this double helix (Figure 14) again features plateau areas. It is while on this plateau region that the non-rigid chain of the double helix is seen to interact with chains in other cells. One sulphate group was seen to be about 7.2 Å away from the hydroxy group of a chain in a neighbouring cell after five picoseconds of the simulation (a temperature of 304 K), so there could be possible electrostatic interaction, given how close that the molecules are getting to each other at times. At the end of the plateau, there is possible interaction near the middle of the chains (the distance between the chains is about 4.5 Å after twenty-six picoseconds), (Figure 15).

The six monomer double helix results indicate that this chain is slightly less stable than the eight monomer double helix. Analysis of the simulation shows that the chain is still a double helix after two picoseconds of simulation, but at three picoseconds (a temperature of 308K), the chain starts to unwind to form a random chain. By fifteen picoseconds, almost half of the chain has unwound, while the other half is still in a helical conformation. The time-energy plot (Figure 16) for this chain shows that the plateau regions present in the eight monomer double helix are again present for the six monomer double helix. At the beginning of this plateau, after eighteen picoseconds of simulation, a little over half of the chain had unravelled to a coil. The temperature at this stage is 309 K. The coil begins to form a helix again after

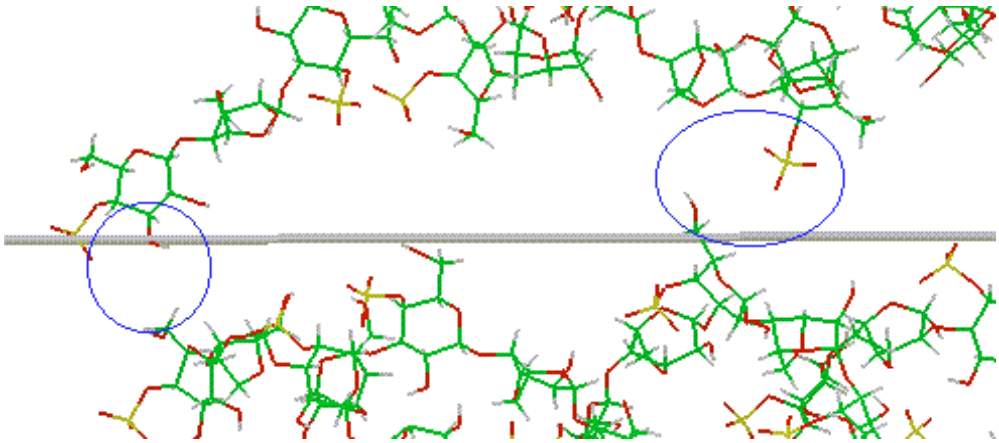

Figure 15 *Possible interactions (circled) between double helices for the eight monomer double helix, after twenty-four picoseconds of simulation*

twenty-two picoseconds, at a temperature of 306 K, and by twenty eight picoseconds, the temperature of the system is 300 K, and about half of the coil had formed a helix again. For the rest of the simulation, no more than half of the chain was in the form of a helix, and little change in conformation was observed. At the end of the simulation, about half of the structure was in the form of a helix, and the other half was in the form of a random coil.

During the simulation, the coil was able to enter other neighbouring cells and was seen to get close enough to other image molecules to possibly interact with them. Some examples of these interactions follow: After six picoseconds of simulation a possible interaction is observed..The interaction can be seen in Figure 17, the two hydroxy groups circled are about 2.5 Å apart, and show that hydrogen bonds between the helices via the hydroxy groups may be possible. Snapshots of other parts of the simulation show that there is also possible interaction between the sulphate groups and the hydroxy group. This could potentially be a much stronger interaction than the interaction between two hydroxy groups, as the sulphate group is more negatively charged than the oxygen atom in the hydroxy groups. Figure 18 shows one such possible interaction, which occurred after twenty-five picoseconds of simulation. The temperature at this point was 296 K. the distance between the oxygen closest to the hydroxy group (from the sulphate group) to the hydrogen in the hydroxy group was measured to be about 4.9 Å.

There are other instances during the simulation where interactions between helices from different cells were possible for the six monomer double helix chain and the eight monomer double helix chain. Some of these are shown in the appendices. Lack of specific water molecules makes it difficult to come to a definite conclusion as to whether there would be interactions between the chains, as the solvent molecules could hinder interactions by hydrogen bonding to the chains, or via steric effects.

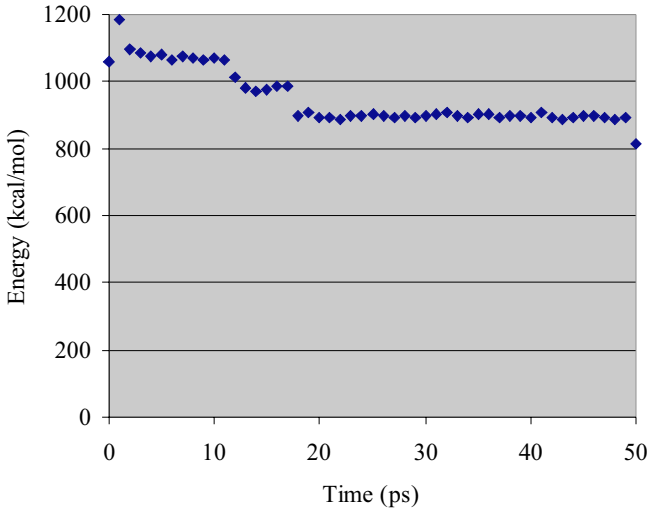

Figure 16 *The time-energy plot for the six monomer double helix*

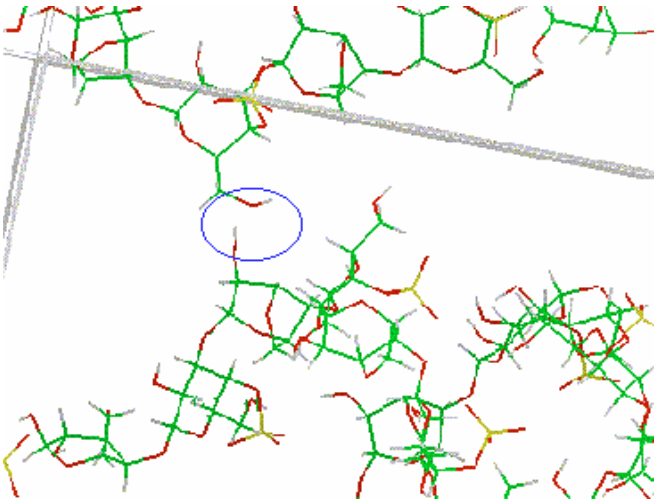

Figure 17 *A possible interaction between two hydroxy groups. The cell boundary can also be seen The blue circle indicates the hydroxy groups that may be interacting*

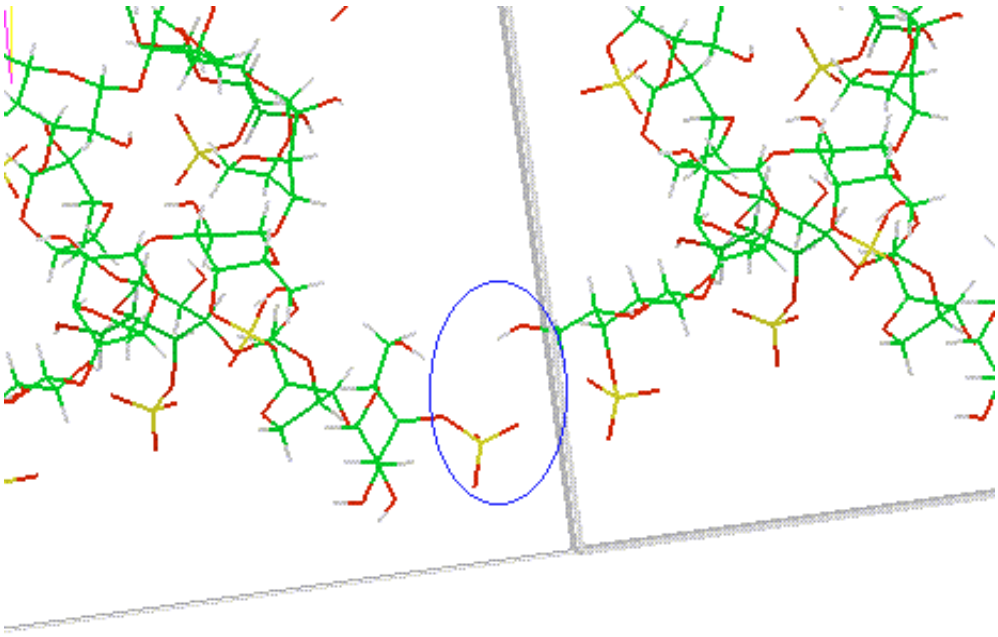

Figure 18 *A possible interaction between a sulphate group and a hydroxy group (circled in blue). This interaction is between six monomer double helices from neighbouring cells, and occurred after twenty-five picoseconds of simulation*

In summary, there is a difference in the behaviour between single helix models simulated with periodic boundary conditions and double helical models also simulated with periodic boundary conditions. In the single helix models, the helical conformation is lost early in the simulation with a preference shown for models with a bend in the centre. This bend may be caused by the packing of other chains around the single helical chain owing to the periodic boundary conditions as a 'free' model without the periodic boundary conditions forms a random coil. The fixed chain in the double helical simulations causes a constraint to the conformation of the movable helical chain, such that the double helical conformation is held in the centre of the chain and the 'ends' unravel. This behaviour is also shown in simulations of double helices without periodic boundary conditions. However, there is a dependence on the number of monomers in the double helical chain with the time taken for the double helical conformation to be lost. This dependence scales in the order; eight monomers takes longer to unravel than six monomers. Hence, there is an indication of a minimum length for stability of a carrageenan double helix.

Conclusion

The results of the simulations have shown that the longer carrageenan chains are more stable than the shorter ones, and that the double helices are quite stable, and can interact with each other. The sulphate groups are said to be a hindrance to aggregation of the double helices, as they can interact with the water molecules and enter into solution easily. Lack of these water molecules in the simulations meant that these interactions were not seen, and so one must model the system with explicit water molecules. A report by Astley et al. [24], indicates that the inclusion of explicit water molecules in simulations of mannopyranose results in structuring of the water which is consistent with the observed sweetness and offers the promise of more consistent results when such simulations become feasible on large scale systems like the ones in this work. Furthermore, cations such as potassium ions are known to promote gelation of carrageenan. This could be because interactions with the negative sulphate groups would be stronger than the hydrogen bonds between water and the sulphate groups. It has been proposed that the binding site for the ions are the ether oxygen atoms and the hydroxy groups, as these are known to be good ligands to cations 25] The sulphate groups are not thought to be involved in the binding of the ions, except in that they can create an electrostatic surface potential [25,26]. However, the IR spectra of various ion forms of carrageenans have been taken to suggest that the sulphate groups are involved in the binding site [27] The proposal that the cations bind with the ether oxygen atoms and the hydroxy groups, but not with the sulphate groups could suggest that the gels formed by carrageenans containing cations are weaker than those formed by agars. Sulphate groups are said to enter solution easily, which would hinder the aggregation of the helices and the gelation mechanism. The sulphate groups entering solution may counteract the effects of the cations (such as potassium ions) binding to the helices causing the aggregation and gelation, thus leading to a weaker gel. The system may then reach an equilibrium between the kinetic and thermodynamic factors. The potassium ions are thought to sit in between helices and bring them together, in the manner proposed by Anderson, Rees et al. [10], and found by Larwood et al. [12] during modelling stud-

ies on gellan. Therefore, modelling these interactions could be useful, as would a study of the kinetic and thermodynamic factors of the gelation mechanism.

The effects of the sulphate groups on the conformation of the helices may be seen by the angles of φ and ψ explored during the simulations by the AG and GA linkages. It has been observed that the molecule can explore a greater area of conformational space about the GA link than the AG link. This could be due to steric hindrance caused by the bulky sulphate group near the AG link. The sulphate group is further away from the GA link than it is from the AG link, and this fact may provide a possible explanation for the relatively unhindered movement about the GA link compared to the AG link. The results have also shown that the conformational space for the AG linkages, as well as the GA linkages vary between different lengths of the polysaccharide chain.

References

1. Guthrie, R.D.; Honeyman, J. *Introduction To Carbohydrate Chemistry*, 4th ed; Clarendon Press: Oxford, 1974.
2. McMurry, J. *Organic Chemistry*, 3rd ed; Brooks And Cole: London, 1992.
3. Aspinall, G.O. *Polysaccharides*, Pergamon Press: Orleans and London, 1970, Vol. 2.
4. Stanley, N. F. In *Food Gels*; Harris, P., Ed.; Elsevier Applied Science: London and New York, 1990.
5. Percival,E. In *Modern Approaches To The Taxonomy Of Red Algae And Brown Algae*; Irvine, D. E. G.; Price, J. H., Eds.; Academic Press: London, 1978.
6. Rees, D. A.; Arnott, S.; Scott, W. E.; McNab, C. G. A. *J. Mol. Biol*, **1974**, *90*, 253.
7. Morris, E. R.; Rees, D. A.; Norton, I. T.; Goodall, D. M. *Carbohyd. Res*, **1980**, *80*, 317.
8. Viebke, C.; Piculell, L.; Nilsson, S. *Macromolecules*, **1994**, *27*, 4160.
9. Plashchina, I. G.; Muratalieva, I. R.; Braudo, E. E.; Tolstoguzov, V. B. *Carbohydrate Polym.* **1986**, *6*, 15.
10. Anderson, N. S.; Campbell, J. W.; Harding, M. M.; Rees, D. A.; Samuel, J. W. B., *J. Mol. Biol*, **1969**, *45*, 85.
11. Rees, D. A. *Chemistry and Industry*, **1972**, 630.
12. Larwood, V. L.; Howlin, B. J.; Webb, G. A. *J. Mol. Model.*, **1996**, *2*, 175.
13. Haggett, N. M. W.; Hoffmann, R. A.; Howlin, B. J.; Webb, G. A. *J. Mol. Model.*, **1997**, *3*, 301.
14. Kawakami, J.; Kawakami, Y.; Nakamura, K.; Kojima, H.; Ito, S.; Tamai, Y. *Glycoconjugate J.* **1998**, *15*, 107.
15. Kozar, T.; Tvaroska, I.; Carver, J.P. *Glycoconjugate Journal* **1998**, *15*, 187.
16. Bohne, A.; Lang, E.; von der Lieth, C.W. *J. Mol. Model.* **1998**, *4*, 33.
17. INSIGHTII and DISCOVER are copyright of Molecular Simulations Inc., San Diego, USA.
18. Homans, S. *Biochemistry*, **1990**, *29*, 9110.
19. Gruza, J.; Koca, J.; Perez, S.; Imberty, A. *J. Mol. Struct. (Theochem)* **1998**, *424*, 269.
20. Martín-Pastor, M.; Espinosa, J. F.; Asensio, J. L.; Jimenez-Barbero, J. *Carbohydr. Res.* **1997**, *298*, 1-2, 15.
21. Verlet, L. *Physical Review*, **1967**, *159*, 98.
22. Gilleron, M.; Siebert, H. C.; Kaltner, H.; von der Lieth, C. W.; Kozar, T.; Halkes, K. M.; Korchagina, E. Y.; Bovin, N. V.; Gabius, H. J.; Vliegenthart, J. F. G. *Eur. J. Biochem.* **1998**, *252*, 3, 416.
23. Ramachandran, G. N.; Ramakrishnan, C.; Sasisekharan, V. *J. Mol. Biol.*, **1963**, *7*, 95.
24. Astley, T.; Birch, G. G.; Drew, M. G. B.; Rodger, P. M.; Wilden, G. R. H. *Food Chem.* **1996**, *56*, 3, 231.
25. Nilsson, S.; Piculell, L. *Macromolecules*, **1991**, *24*, 3804.
26. Belton, P. S.; Goodfellow, B. J.; Wilson, R. H. *Macromolecules*, **1989**, *22*, 1636.
27. Norton, I. T.; Goodall, D. M.; Morris, E. R.; Rees, D. A. *J. Chem. Soc., Faraday Trans.*, **1983**, *79*, 2475.

Appendix 1

AG link contour plots

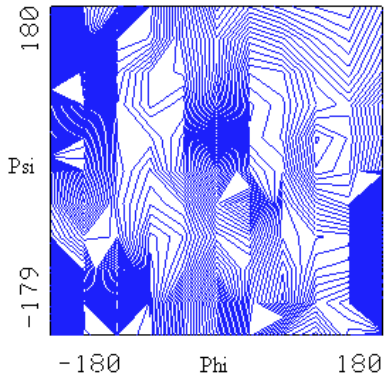

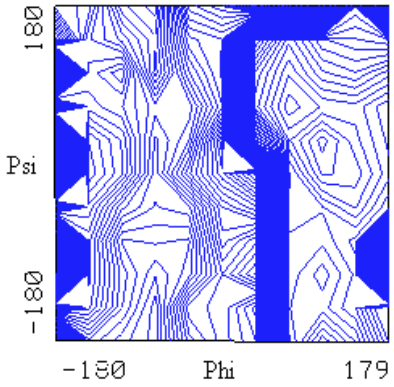

The plots for the AG link in the eight monomer helix. The top diagram shows the contour plot, and the bottom diagram shows a 3D surface representation of the contour plot. The vertical axis represents the total energy of the chain. Note phi and psi are oriented the same way as in the contour plot.

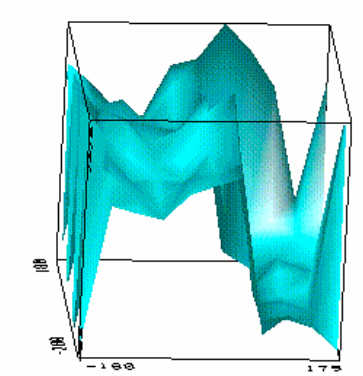

The 3D surface representation for the AG link in the six monomer chain.

Appendix 2

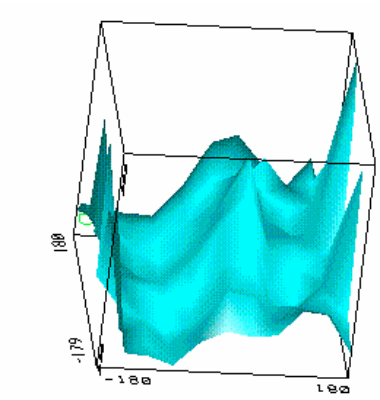

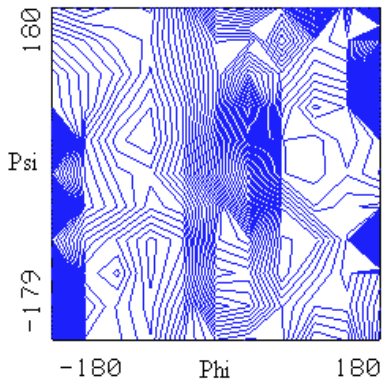

The plots for the AG link in the three monomer helix. The bottom diagram shows the contour plot, and the top diagram shows a 3D surface representation of the contour plot. The vertical axis represents the total energy of the chain. Note phi and psi are oriented the same way as in the contour plot i.e. the horizontal axis in the 3D plot refers to phi etc.

Appendix 3

The GA link

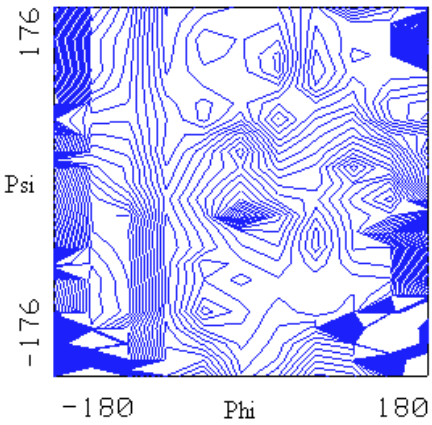

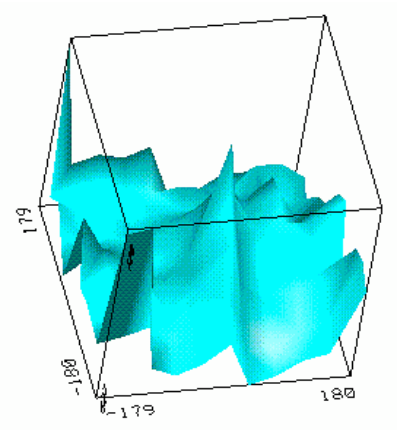

The contour plot for the GA link for the six monomer helix along with the 3D surface representation.

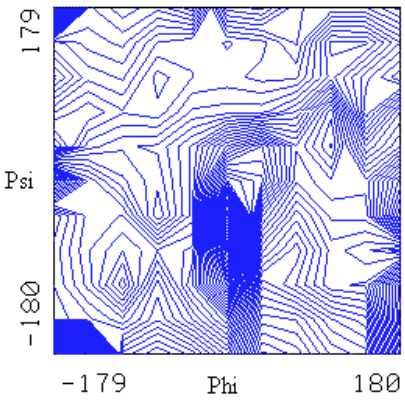

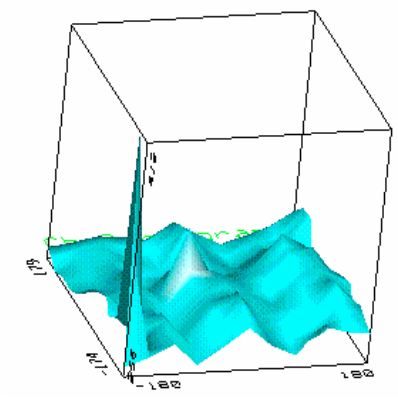

The contour plot for the GA link for the three monomer helix along with the 3D surface representation

Appendix 4

Ramachandran plots (Phi and Psi values are in degrees)

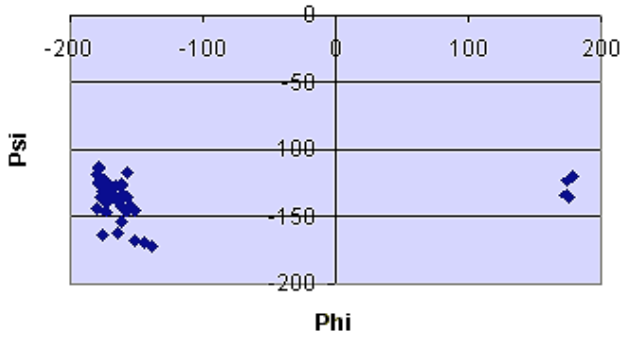

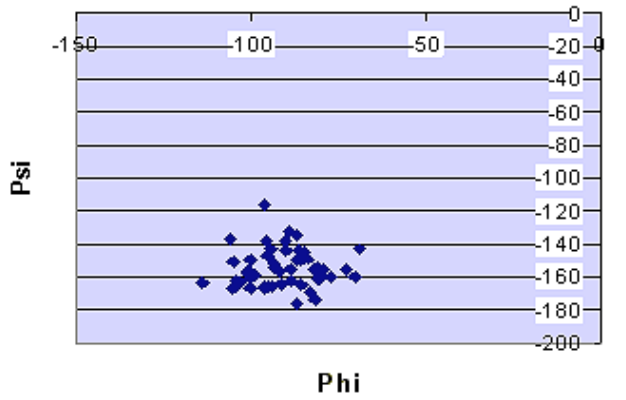

Appendix 5

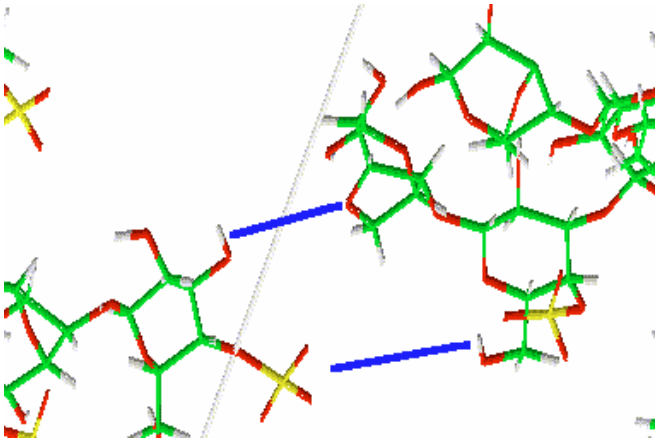

Possible interactions in the six monomer chains under PBC

A possible interaction after six picoseconds of dynamics, indicated by the blue line. This is between the hydroxy hydrogen atom and the ether oxygen atom. Also there is a possible interaction between the sulphate group and the hydroxy group, as shown above. This is for the double helix.

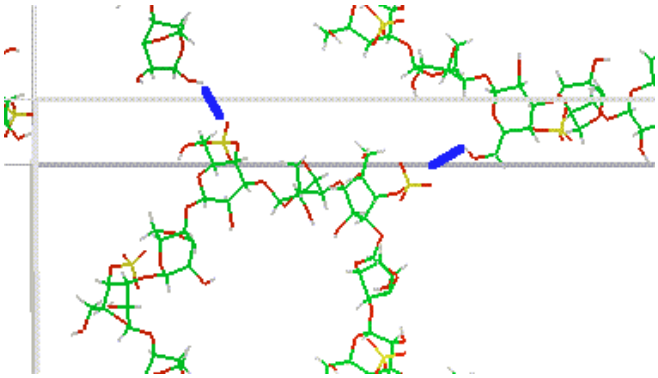

Two possible interactions are shown here. The picture is of the single six monomer helix simulated under PBC, after thirteen picoseconds of simulation.